FOUNDATIONS
ADVANCES

Volume 77 (2021)

Supporting information for article:

Improvement of precision in refinements of structure factors using convergent-beam electron diffraction patterns taken at Bragg-excited conditions

B. Aryal, D. Morikawa, K. Tsuda and M. Terauchi

Convergence test

The number of reflections necessary for the dynamical calculations were determined from convergence test of eigen values of three representative Bloch states at [100] incidence. Changes in eigen values with changes in excitation error were calculated. The percentage change in eigen values of these Bloch states were found to be less than one percent for $s_g \geq 0.09$ Å^{-1}. The result of the convergence test is shown in Fig. (S1). The reflections with excitation error $s_g < 0.10$ Å^{-1} were used for the dynamical calculations, and those with $0.10 < s_g < 0.11$ Å^{-1} were treated by perturbation. In the present analysis, 701 reflections were used for the dynamical calculations and 52 reflections were treated by perturbation. The number of reflections used for simulations were 701 at [100], 613 at [110], and 502 at [111], respectively.

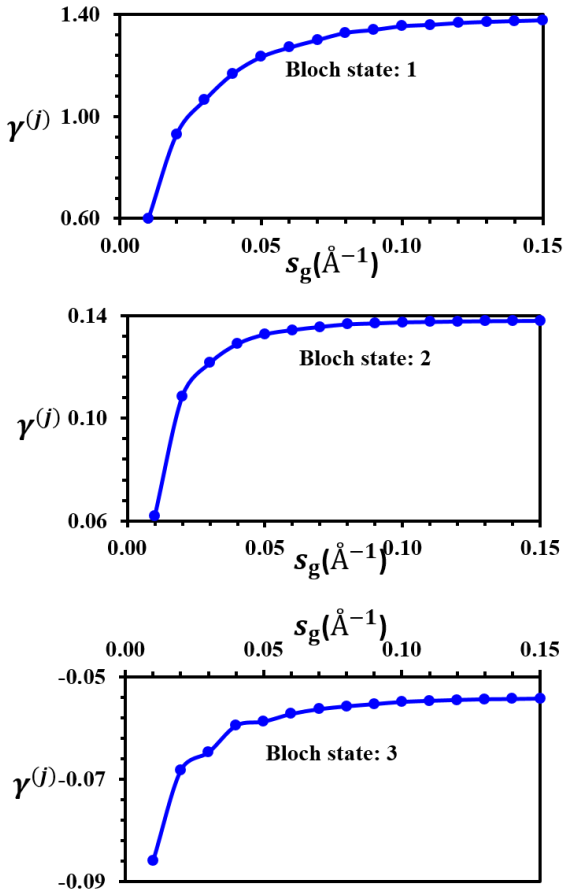

Fig. S1: Plot showing changes in eigen values with changes in excitation error for three representative Bloch states at [100] incidence.

Determination of the best tilting conditions

To check the influence of scattering geometry on sensitivity of CBED patterns, sen sitivity was examined using CBED patterns simulated at different incidences and Bragg-excited conditions. Changes in GOF were calculated by changing IAM struc ture factors of the 001, 011, $\bar{1}11$, 002 and 021 reflections in the range -5% to 5 %. The results are shown in Figs. S2(a-e). From simulated result shown in Fig. S2 (a-e), it was confirmed that 001, 002, $\bar{1}11$ Bragg-excited patterns near [110] and 011 and 021 Bragg-excited patterns near [100] show higher sensitivity to the respective structure factors. It was also found that sensitivity of CBED patterns depend on scat-tering geometry and crystal orientation. Experimental CBED patterns taken at the Bragg-excited conditions as stated above have been used in this analysis.

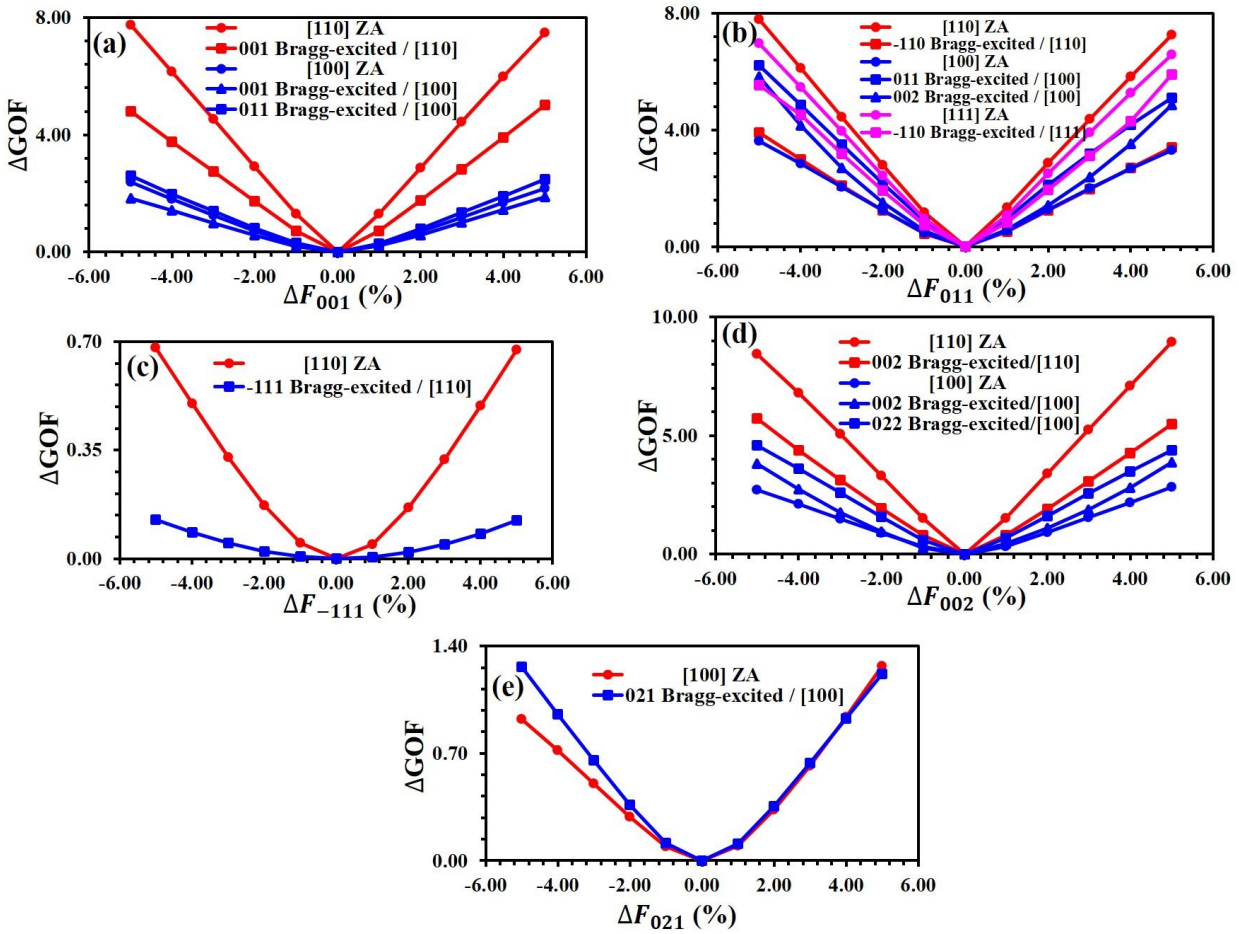

Fig. S2. Plot showing changes in GOF with changes in IAM structure factor of the (a) 001, (b) 011, (c) $\bar{1}11$, (d) 002 and (e) 021 reflections for CBED patterns simulated at [100], [110] and [111] incidences and different Bragg-excited conditions near these incidences.

Influence of the TDS signals

First-order Laue zone (FOLZ) reflections of experimental CBED patterns taken from thicker specimen positions showed much broader intensities compared to the calculated ones. As an example, part of the fitting result of FOLZ reflections of [100] incidence CBED patterns taken from two positions of same segment with thickness ~ 1295 Å and ~ 535 Å is shown in Fig. (S3). Inelastic background intensity owing to the remaining thermal diffuse scattering (TDS) signal could be the origin of this effect. In KTO, tantalum atom located at body centered position has a larger absorption coefficient. To reduce absorption effects and inelastic background intensity, CBED patterns taken in the thickness range 650 to 950 Å were used in this analysis.

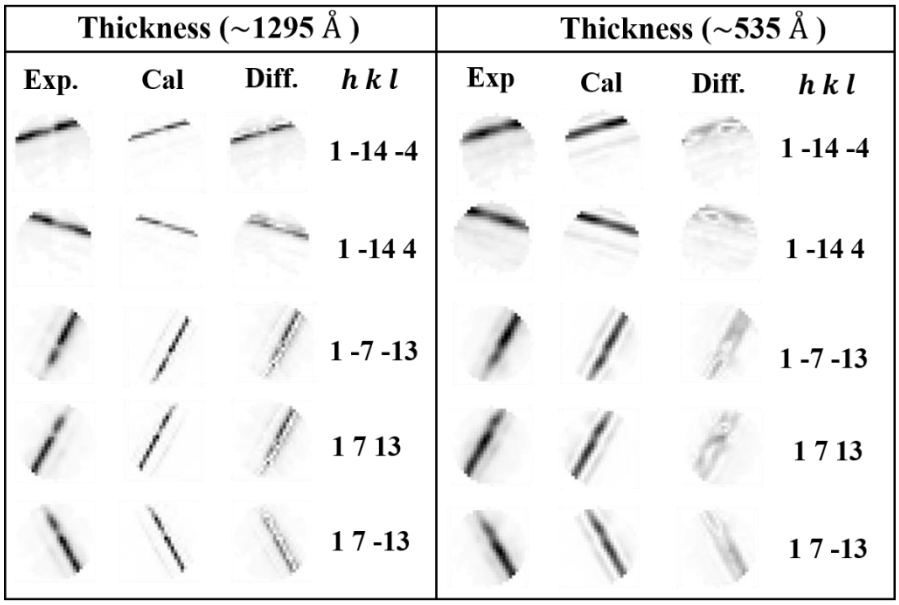

Fig. S3: Part of the fitting result of FOLZ reflections of two [100] incidence CBED patterns taken from two positions of same segments with thickness ~ 1295 Å and ~ 535 Å. The patterns in the left, center, and right columns show experimental, calculated, and difference intensities of the CBED discs, respectively.

Final results of fitting (FOLZ reflections)

Atomic displacement parameters (ADPs) were refined using zeroth-order Laue zone (ZOLZ) and FOLZ reflections of CBED patterns taken at three ZA and five Bragg-excited conditions. Final results of fitting of all the FOLZ reflections of CBED patterns taken at [100] incidence and $01\bar{1}$ Bragg-excited condition near [100] are shown in Fig. (S4) and Fig. (S5).

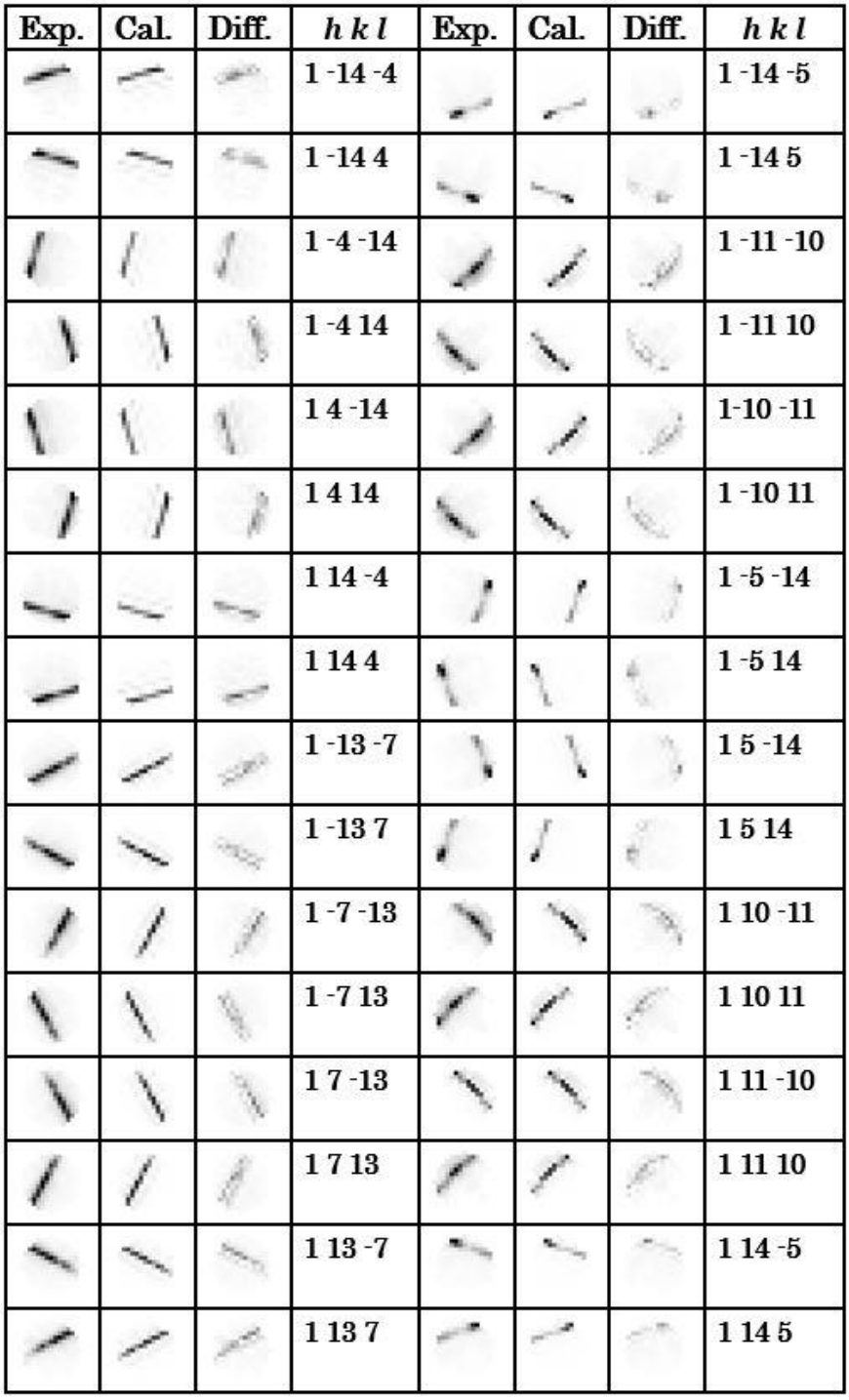

Fig. S4. Final results of fitting of FOLZ reflections of [100] incidence CBED pattern. The patterns in the left, center and right columns show experimental, calculated and difference intensities of the CBED discs, respectively.

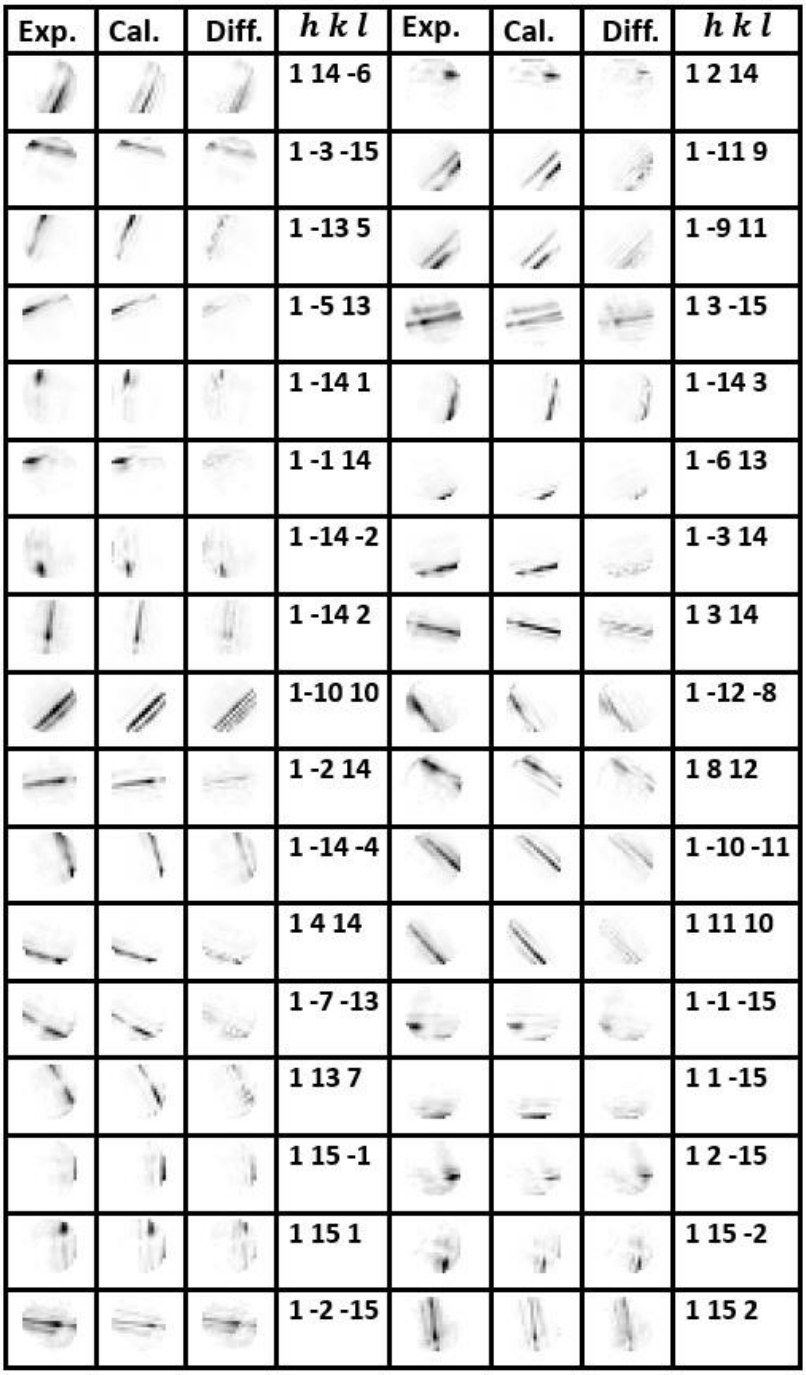

Fig. S5. Final results of fitting of FOLZ reflections of the CBED pattern taken at $01\bar{1}$ Bragg-excited condition near [100]. The patterns in the left, center and right columns show experimental, calculated and difference intensities of the CBED discs, respectively.

Sensitivities of CBED patterns to the changes in ADPs

The sensitivities of ZA and Bragg-excited CBED patterns to the changes in ADPs of potassium, tantalum and oxygen atoms were investigated. The changes in goodness-of-fit (GOF) with changes in isotropic ADPs of potassium, tantalum and oxygen atoms were calculated. This is shown in Fig. (S6). Both ZA and Bragg-excited CBED patterns show larger change in GOF with changes in atomic-displacement parameter (ADP) of tantalum atom. Changes in GOF with changes in ADP of the oxygen atom is smaller for both of these patterns. Present result suggests lower sensitivity of ZA and Bragg-excited CBED patterns to the changes of ADP of oxygen atom.

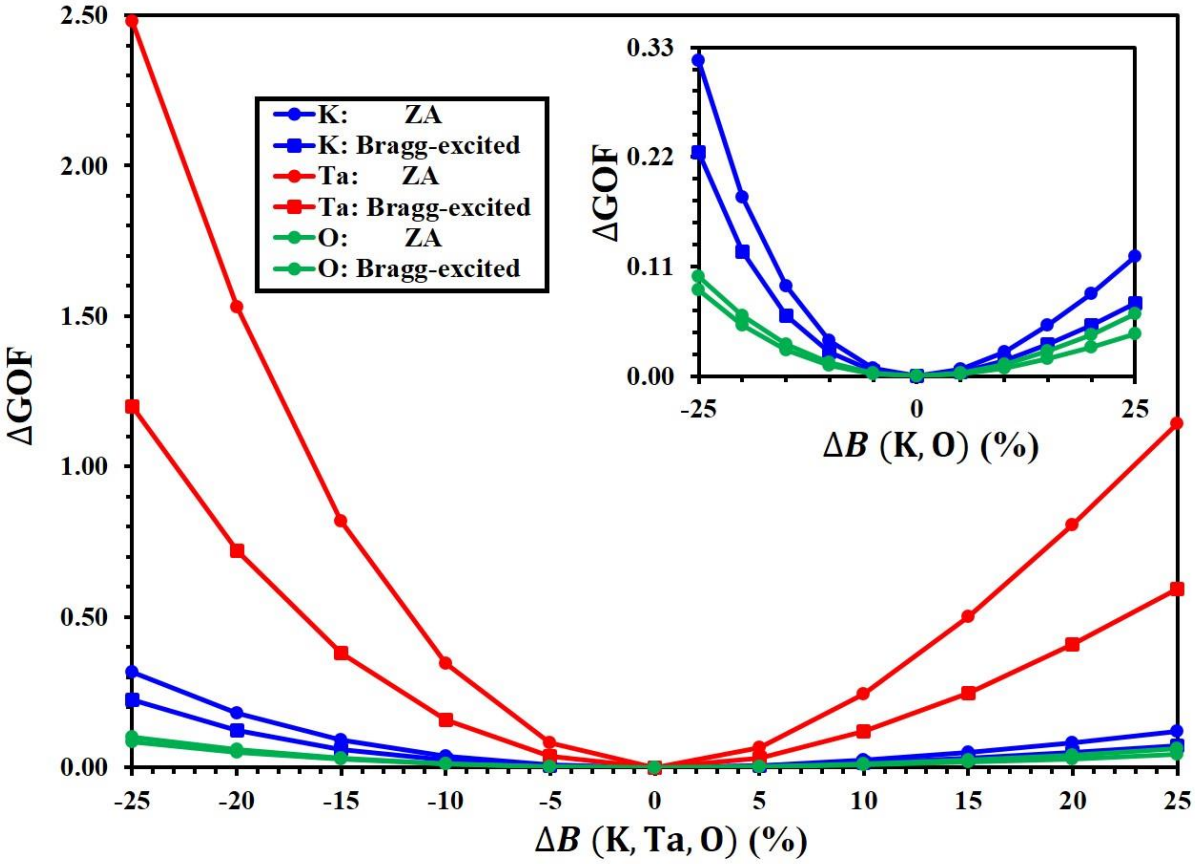

Fig. S6. Plot showing the changes in GOF with changes in isotropic ADPs of potassium, tantalum and oxygen atoms. Results for potassium and oxygen atoms are separately shown in an inset to emphasize the difference.

Final results of fitting (ZOLZ reflections)

Low-order structure factors were refined using zeroth-order Laue zone (ZOLZ) and FOLZ reflections of CBED patterns taken at three ZA and five Bragg-excited conditions. Final results of fitting of all ZOLZ reflections of CBED patterns taken at [100] incidence and $01\bar{1}$ Bragg-excited condition near [100] are shown in Fig. (S7) and Fig. (S8).

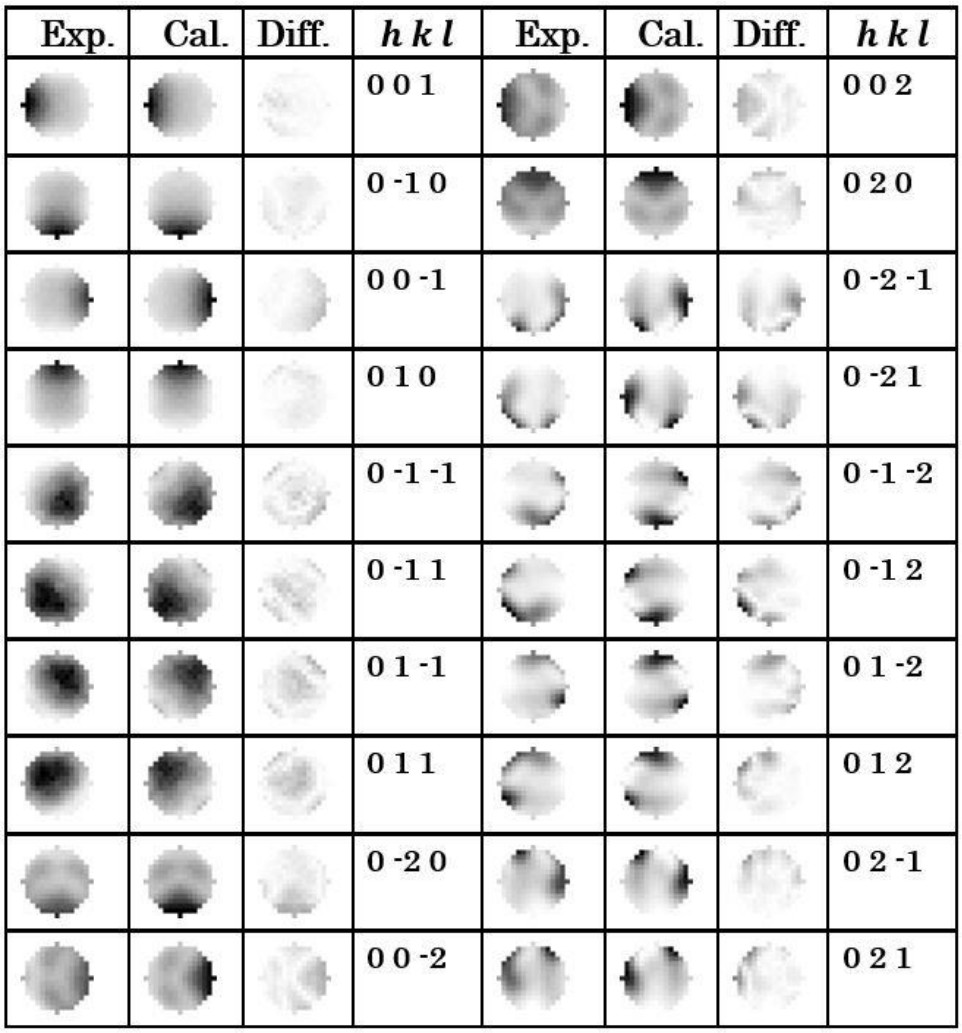

Fig. S7. Final results of fitting of ZOLZ reflections of [100] incidence CBED pattern. The patterns in the left, center and right columns show experimental, calculated and difference intensities of the CBED discs, respectively.

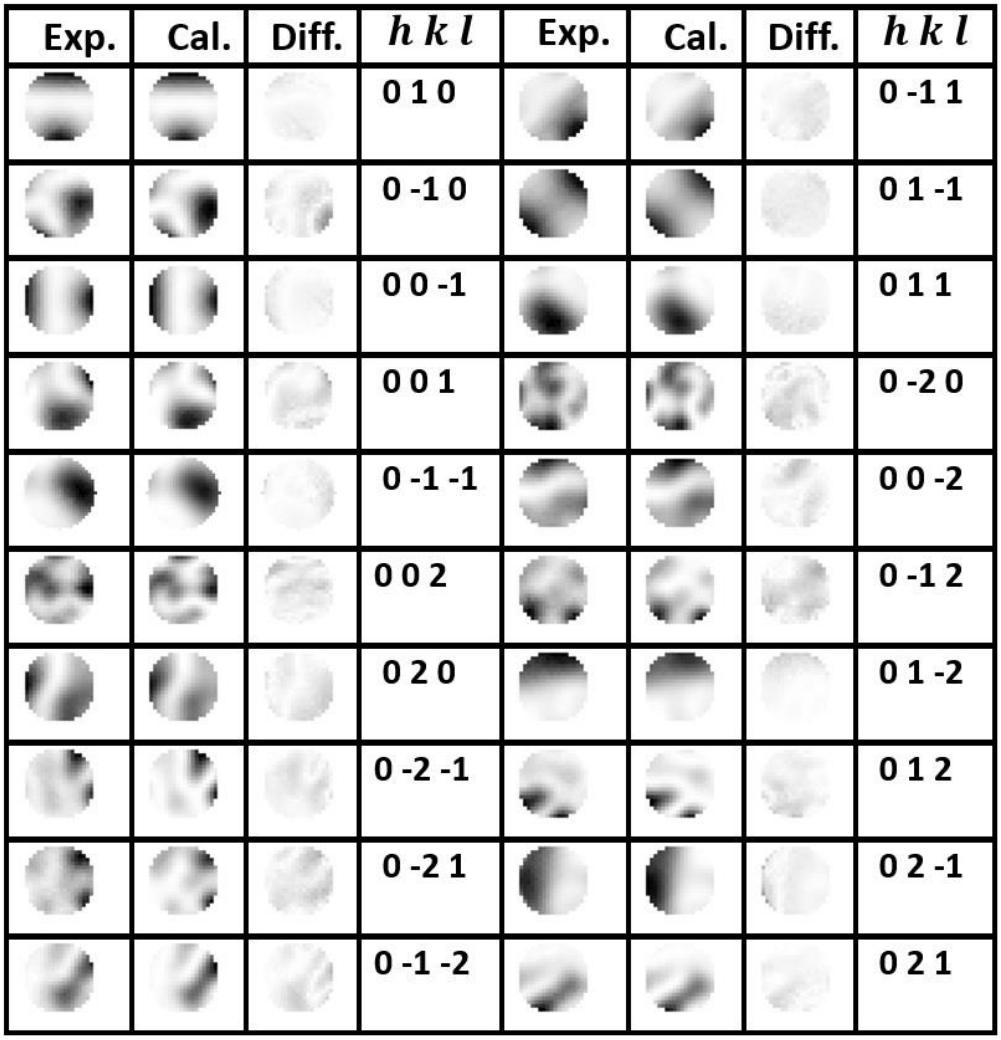

Fig. S8. Final results of fitting of ZOLZ reflections of the CBED pattern taken at $01\bar{1}$ Bragg-excited condition near [100]. The patterns in the left, center and right columns show experimental, calculated and difference intensities of the CBED discs, respectively.

Correlation coefficients

The result of sensitivity analysis could not explain the origin of higher precision of Bragg-excited CBED patterns for the determination of low-order structure factors. To find the origin of higher precision, correlation coefficient between the refined low-order structure factors were examined. Their values are shown in table I. The correlation coefficients between the refined structure factors are larger in the refinement using ZA patterns than using Bragg-excited patterns.

Structure factors	Correlation coefficients	
	Zone-axis	Bragg-excited
$F_{00\bar{1}}$ and $F_{01\bar{1}}$	-0.29	-0.19
$F_{00\bar{1}}$ and $F_{1\bar{1}\,\bar{1}}$	0.56	0.13
$F_{00\bar{1}}$ and $F_{00\bar{2}}$	0.18	0.08
$F_{00\bar{1}}$ and $F_{0\bar{2}\,\bar{1}}$	-0.04	-0.01
$F_{01\bar{1}}$ and $F_{1\bar{1}\,\bar{1}}$	0.46	0.20
$F_{01\bar{1}}$ and $F_{00\bar{2}}$	-0.38	-0.18
$F_{01\bar{1}}$ and $F_{0\bar{2}\,\bar{1}}$	0.53	0.28
$F_{1\bar{1}\,\bar{1}}$ and $F_{00\bar{2}}$	-0.78	-0.14
$F_{1\bar{1}\,\bar{1}}$ and $F_{0\bar{2}\,\bar{1}}$	-0.08	-0.05
$F_{00\bar{2}}$ and $F_{0\bar{2}\,\bar{1}}$	-0.28	-0.11